AGU PUBLICATIONS

JGR

Journal of Geophysical Research: Space Physics

RESEARCH ARTICLE
10.1002/2014JA019789

Key Points:
- Verify existence of ULF electromagnetic phenomena preceding large earthquakes
- ULF geomagnetic anomalies are more sensitive to larger and closer events
- ULF seismomagnetic phenomena obtained at KAK do contain precursory information

Correspondence to:
K. Hattori,
hattori@earth.s.chiba-u.ac.jp

Citation:
Han, P., K. Hattori, M. Hirokawa, J. Zhuang, C.-H. Chen, F. Febriani, H. Yamaguchi, C. Yoshino, J.-Y. Liu, and S. Yoshida (2014), Statistical analysis of ULF seismomagnetic phenomena at Kakioka, Japan, during 2001–2010, *J. Geophys. Res. Space Physics*, *119*, 4998–5011, doi:10.1002/2014JA019789.

Received 15 JAN 2014
Accepted 20 MAY 2014
Accepted article online 26 MAY 2014
Published online 16 JUN 2014

Statistical analysis of ULF seismomagnetic phenomena at Kakioka, Japan, during 2001–2010

Peng Han[1], Katsumi Hattori[1], Maiko Hirokawa[1], Jiancang Zhuang[2], Chieh-Hung Chen[3], Febty Febriani[1], Hiroki Yamaguchi[1], Chie Yoshino[1], Jann-Yenq Liu[4,5], and Shuji Yoshida[1]

[1]Graduate School of Science, Chiba University, Chiba, Japan, [2]Institute of Statistical Mathematics, Tokyo, Japan, [3]Department of Earth and Environmental Sciences, National Chung Cheng University, Chiayi, Taiwan, [4]Institute of Space Science, National Central University, Chung-Li, Taiwan, [5]Center for Space and Remote Sensing Research, National Central University, Chung-Li, Taiwan

Abstract To clarify and verify the ultralow frequency (ULF) seismomagnetic phenomena, we have performed statistical studies on the geomagnetic data observed at the Kakioka (KAK) station, Japan, during 2001–2010. We investigated the energy of ULF geomagnetic signals of the frequency around 0.01 Hz using wavelet transform analysis. To minimize the influences of artificial noises and global geomagnetic perturbations, we used only the geomagnetic data observed at nighttime (LT 2:30 A.M. to 4:00 A.M.) and utilized observations from a remote station, Kanoya, as a reference. Statistical results of superposed epoch analysis have indicated that ULF magnetic anomalies are more likely to appear before sizable earthquake events ($E_s > 10^8$) rather than after them, especially 6–15 days before the events. Further statistical investigations show clearly that the ULF geomagnetic anomalies at KAK station are more sensitive to larger and closer events. Finally, we have evaluated the precursory information of ULF geomagnetic signals for local sizable earthquakes using Molchan's error diagram. The probability gain is around 1.6 against a Poisson model. The above results have indicated that the ULF seismomagnetic phenomena at KAK clearly contain precursory information and have a possibility of improving the forecasting of large earthquakes.

1. Introduction

During the past few decades, electromagnetic variations associated with earthquakes and volcanic activities have been intensively studied [e.g., *Johnston*, 1997; *Hayakawa*, 1999; *Hayakawa and Molchanov*, 2002; *Hattori*, 2004]. So far, there have been many reports on the seismoelectromagnetic phenomena recorded by different measurements covering a very wide frequency range all over the world. These measurements can be classified into three types: (1) passive ground-based observation for lithospheric emissions in the frequency range from DC to VHF [*Varotsos and Alexopoulos*, 1984; *Varotsos and Lazaridou*, 1991; *Fraser-Smith et al.*, 1990; *Molchanov et al.*, 1992; *Kopytenko et al.*, 1993, 1994, 2006; *Lighthill*, 1996; *Hayakawa et al.*, 1996a; *Kawate et al.*, 1998; *Nagao et al.*, 2002; *Uyeda et al.*, 2002, 2009; *Hattori*, 2004; *Hattori et al.*, 2004a, 2004b; *Telesca and Hattori*, 2007; *Telesca et al.*, 2008; *Han et al.*, 2009; *Chavez et al.*, 2010; *Hirano and Hattori*, 2011; *Huang*, 2011a, 2011b; *Wen et al.*, 2012; *Xu et al.*, 2013]; (2) active ground-based monitoring of seismoatmospheric and seismoionospheric perturbations utilizing transmitter signals [*Gokhberg et al.*, 1982; *Hayakawa et al.*, 1996b; *Molchanov and Hayakawa*, 1998; *Liu et al.*, 2001, 2006, 2009; *Kon et al.*, 2011]; and (3) satellite observations of plasma perturbations, radio emissions, and thermal anomalies associated with earthquakes in the upper atmosphere [*Galperin and Hayakawa*, 1996; *Tramutoli et al.*, 2005; *Ouzounov et al.*, 2006, 2007; *Sarkar et al.*, 2007; *Akhoondzadeh et al.*, 2010].

Recently, ultralow frequency (ULF, less than 1 Hz) has been considered as a prospective band in search of earthquake precursory signatures because of its larger skin depth [*Fraser-Smith et al.*, 1990; *Hattori*, 2004; *Hattori et al.*, 2004a, 2004b; *Yen et al.*, 2004; *Liu et al.*, 2006; *Telesca et al.*, 2008; *Zhao et al.*, 2009; *Chen et al.*, 2010, 2013; *Hirano and Hattori*, 2011; *Wen et al.*, 2012; *Han*, 2013; *Xu et al.*, 2013]. Furthermore, abundant indoor and/or outdoor experiments and numerical simulations have confirmed the existence of ULF seismoelectromagnetic phenomena [*Molchanov and Hayakawa*, 1995; *Yoshida et al.*, 1997; *Freund*, 2000, 2002; *Huang*, 2002, 2005; *Huang and Lin*, 2010; *Enomoto*, 2012; *Ren et al.*, 2012]. However, it is still considerably

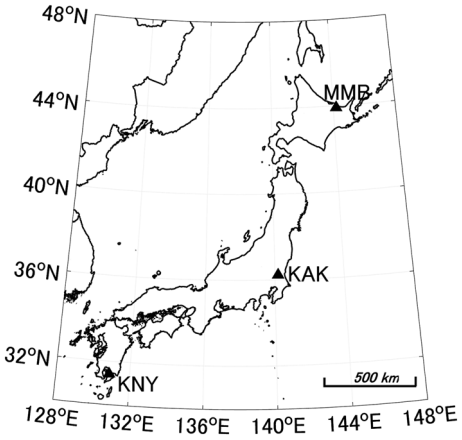

Figure 1. Locations of geomagnetic stations in Table 1.

difficult to understand the relationship between the observed results and the physical mechanisms clearly, and there are active debates on the linkage between seismoelectromagnetic phenomena and earthquakes in the geophysical community [*Campbell*, 2009; *Thomas et al*., 2009; *Kappler et al*., 2010; *Masci*, 2010].

In order to verify the existence of ULF electromagnetic phenomena preceding large earthquakes, *Hattori et al.* [2013a] have recently analyzed the geomagnetic data observed by a network in Kanto, Japan, during 2000–2010 as a case study. Their results indicated that there were statistical significances of regional ULF geomagnetic anomalies from a few days to a few weeks prior to sizable earthquakes. To validate their results and to find out the characteristics of ULF seismomagnetic phenomena in other regions, we apply some statistical studies based on the data of Kakioka (KAK) station, Japan, during 2001–2010 in this study.

2. Geomagnetic Observations and Studied Earthquakes

It is essential to evaluate the statistical significance of the precursory information of preseismic phenomena, since these phenomena are neither always observed or detected before all large earthquakes nor always followed by large earthquakes. For the statistical study of ULF seismomagnetic phenomena, the following two preconditions are required: (1) a long-term continuous monitoring of ULF magnetic field and (2) a sufficient number of sizable earthquakes. With a superb quality and long-term continuity of data, three JMA (Japan Meteorological Agency) observatories, Memambetsu (MMB), KAK, and Kanoya (KNY) provide an excellent opportunity for carrying out such an analysis. Figure 1 shows the locations of these three stations, and Table 1 lists more details of them. In this study, we use the 1 Hz geomagnetic data of these three stations during 2001–2010, which are available on the website of KAK observatory. The reported data are absolute values of the horizontal (H), declination (D), and vertical (Z) components. Here we transform H and D to the X (N-S) and Y (E-W) components.

According to previous studies [*Hattori*, 2004; *Zhuang et al*., 2005; *Schekotov et al*., 2007], the detection of ULF magnetic anomalies seems to depend on the magnitude of the target earthquake and the distance from the geomagnetic station to the hypocenter (hereafter, hypocenter distance). Therefore, in this study we employ the E_s parameter which considers both factors to select earthquake events. The E_s index is the daily sum of the local earthquake energy (E_s') defined by the following formula [*Hattori et al*., 2006]:

$$E_s = \sum_{1\text{day}} E_s' \tag{1}$$

$$E_s' = \frac{10^{4.8+1.5M}}{r^2} \tag{2}$$

where M and r are the magnitude of the earthquake and the hypocenter distance, respectively. In order to compare our present and previous studies, here we adopt the same criterion used by *Hattori et al.* [2013a]: an earthquake event occurs when the E_s index in that day exceeds 10^8. To satisfy this criterion, for an earthquake of magnitude 4.0, the hypocenter distance should be less than 25 km. Note that only shallow earthquakes (less than 60 km deep) are taken into account. There are 3, 6, and 50 events within 100 km (epicenter distance

Table 1. List of ULF Geomagnetic Stations Shown in Figure 1

Station Name (Code)	Geographic Coordinates	Type of Magnetometer	Sampling Rate	Reported Data
Memambetsu (MMB)	43.91°N, 144.19°E	Fluxgate	1 Hz	*H*, *D*, and *Z*
Kakioka (KAK)	36.23°N, 140.12°E	Fluxgate	1 Hz	*H*, *D*, and *Z*
Kanoya (KNY)	31.42°N, 130.88°E	Fluxgate	1 Hz	*H*, *D*, and *Z*

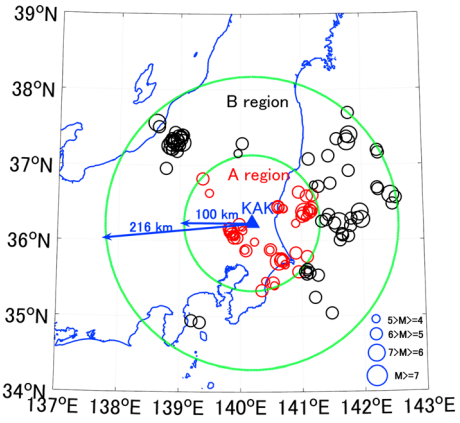

Figure 2. Spatial distributions of major earthquakes with $E_s > 10^8$ around KAK station during 2001–2010. The blue triangle indicates the location of the KAK station. The red and black open circles indicate earthquakes in Regions A and B, respectively. The sizes of circles are scaled to the magnitudes. The green circles demark the outer boundaries of Regions A and B, with radii 100 km and 216 km, respectively.

$R < 100$ km) from MMB, KNY, and KAK stations during 2001–2010, respectively. This study focuses on KAK station, where the earthquake samples are sufficient for a statistical analysis. Here the region within 100 km from KAK station is named Region A. It should be emphasized that the earthquake event is defined by the daily sum of earthquake energy E_s rather than E_s'. Even if there are several adequate earthquakes happening on a same day, we only count it as one single event. Furthermore, to investigate whether there is any distance dependence of seismomagnetic anomalies, we choose another 50 samples with $E_s > 10^8$ in a farther region (Region B) surrounding region A (Figure 2). The earthquake events in Regions A and B are shown in Figure 2, and their detailed information is given in Table 2 and Table 3, respectively. Here we choose 216 km as the outer boundary for Region B, such that there are equal numbers of earthquake events in Regions A and B during 2001–2010.

3. Data Processing

3.1. Signal Discrimination and Wavelet Analysis

Generally, ground-based ULF geomagnetic data are superposition of several signals: global magnetic perturbations, artificial noises, and magnetic signals possibly due to underground activities. Therefore, the key point in seismomagnetic studies is to distinguish the earthquake-related signals from the others. Figure 3 shows a typical spectrogram of the *Z* component of geomagnetic data at KAK station, with clear time zone of lower background noise from midnight to early morning in local time (LT) when the train system is shut down. Thus, to minimize the influences of such artificial noises, we only utilize the data during 02:30–04:00 LT. Note that the artificial noises of MMB and KNY stations are very small even in the daytime, because they are located in the countryside, far away from railways.

In previous studies, one of the most frequently reported periods of seismoelectromagnetic phenomena was around 100 s [*Fraser-Smith et al.*, 1990; *Hayakawa et al.*, 1996a; *Uyeda et al.*, 2002; *Hattori*, 2004; *Hattori et al.*, 2004a, 2004b, 2013a, 2013b; *Han et al.*, 2011]. In this study we apply the wavelet transform to the 1 Hz geomagnetic data and extract the signals at the frequency around 0.01 Hz. After comparison among several types of wavelets, we adopt Daubechies 5 (db5) as the mother wavelet, following *Jach et al.* [2006] who found out that the db5 wavelet is effective. Details of such wavelet analysis are found in *Han et al.* [2011] and *Hattori et al.* [2013a, 2013b]. Figure 4 demonstrates an example of wavelet transform results of the *X* component. It could be seen that the geomagnetic variations at the 100 s period are usually similar among the three stations. Thus, either KNY or MMB can be taken as a reference station in removing global geomagnetic perturbations.

3.2. Daily Energy of Geomagnetic Signals

Early studies have indicated that there are possible energy enhancements of ULF geomagnetic signals in the *Z* component prior to large earthquakes [*Hattori*, 2004; *Hattori et al.*, 2004a, 2013a; *Han et al.*, 2011]. Therefore, this study focuses on the geomagnetic energy variation in the *Z* component and discusses the relationship between the energy enhancements and earthquake activities. First, we apply a six-level discrete wavelet transform using db5 mother wavelet to the daily 1 Hz nighttime geomagnetic data. Next, we extract the detailed signals in the sixth level, where the central frequency is 0.01 Hz. Finally, we compute the daily average energy of the obtained 0.01 Hz signals [see *Hattori et al.*, 2013a for more details].

Figure 5 shows the correlations of 10 year daily energies for each pair of the three stations. Figures 5a–5c show the correlations in *H* component; Figures 5d–5f present the correlations in *Z* component. The correlation coefficients are higher than 0.92 in *H* components for all three pairs of stations, suggesting

Table 2. List of Major Earthquakes With $E_s > 10^8$ in Region A

No.	DDMMYY	Latitude (°N)	Longitude (°E)	Depth (km)	Epicenter Distance (km)	Magnitude (JMA)	E_s' (lg)	E_s (lg)
1	31 March 2001	36.82	139.38	4	97.68	5.2	8.6	8.6
2	25 May 2001	35.76	140.67	47	68.05	5.0	8.5	8.5
3	31 May 2001	36.18	139.81	55	34.48	4.7	8.2	8.3
4	20 July 2001	36.16	139.81	55	34.36	5.0	8.7	8.7
5	3 September 2001	36.39	141.15	49	87.93	4.9	8.1	8.1
6	11 February 2002	35.79	141.09	34	95.17	5.2	8.6	8.6
7	12 February 2002	36.59	141.08	47	89.60	5.7	9.3	9.3
8	4 May 2002	35.46	140.41	31	87.67	4.8	8.1	8.1
9	14 June 2002	36.22	139.98	56	18.83	5.1	8.9	8.9
10	16 October 2002	35.84	140.90	34	78.14	5.0	8.4	8.4
11	21 October 2002	36.37	141.12	49	85.43	5.4	8.9	8.9
12	21 January 2003	36.37	141.03	46	76.98	5.1	8.5	8.5
13	13 March 2003	36.09	139.86	47	33.57	5.0	8.8	8.8
14	8 April 2003	36.07	139.91	47	30.58	4.6	8.2	8.2
15	12 May 2003	35.87	140.09	46	41.35	5.3	9.2	9.2
16	17 May 2003	35.74	140.65	47	68.96	5.3	8.9	8.9
17	9 June 2003	36.42	140.70	54	50.87	4.7	8.1	8.1
18	4 August 2003	36.44	140.61	58	44.87	4.9	8.4	8.4
19	15 November 2003	36.43	141.16	48	90.47	5.8	9.5	9.5
20	11 March 2004	36.32	141.01	47	74.36	5.3	8.9	8.9
21	4 April 2004	36.39	141.15	48	88.50	5.8	9.5	9.5
22	10 July 2004	36.08	139.88	48	31.87	4.7	8.3	8.3
23	16 February 2005	36.04	139.89	46	34.30	5.3	9.2	9.2
24	11 April 2005	35.73	140.62	51	68.45	6.1	10.1	10.1
25	15 May 2005	36.63	139.49	8	76.69	4.8	8.2	8.4
26	20 June 2005	35.73	140.69	50	71.86	5.6	9.3	9.3
27	28 July 2005	36.13	139.85	51	32.71	5.0	8.7	8.7
28	9 September 2005	35.59	140.95	37	98.96	5.0	8.3	8.3
29	16 October 2005	36.04	139.94	47	30.93	5.1	8.9	8.9
30	19 October 2005	36.38	141.04	48	78.58	6.3	10.3	10.3
31	16 November 2005	36.31	141.07	47	79.26	4.8	8.1	8.1
32	28 December 2005	36.18	140.03	53	15.31	4.8	8.5	8.5
33	8 May 2007	36.06	139.89	46	32.74	4.5	8.0	8.0
34	2 June 2007	36.13	140.03	49	17.39	4.6	8.3	8.3
35	16 August 2007	35.44	140.53	30	92.95	5.3	8.8	8.9
36	18 August 2007	35.34	140.35	20	99.90	5.2	8.6	8.7
37	7 October 2007	35.68	140.73	44	78.03	4.8	8.1	8.1
38	30 November 2007	36.43	140.70	52	50.57	4.7	8.1	8.1
39	8 March 2008	36.45	140.61	57	45.38	5.2	8.9	8.9
40	4 April 2008	36.12	139.83	53	34.46	5.0	8.7	8.7
41	25 April 2008	35.68	140.72	48	77.78	4.8	8.1	8.1
42	5 July 2008	36.64	140.95	49	82.37	5.2	8.6	8.6
43	20 August 2008	36.06	139.9	45	32.15	4.6	8.2	8.2
44	22 August 2008	36.44	140.62	55	44.97	5.2	8.9	8.9
45	22 November 2008	35.98	140.23	41	27.92	4.4	8.0	8.0
46	28 April 2009	36.41	141.13	47	86.87	5.0	8.3	8.3
47	23 October 2009	36.60	141.18	45	97.67	5.0	8.2	8.2
48	23 July 2010	35.88	140.49	35	47.62	5.0	8.8	8.8
49	22 September 2010	35.88	140.48	35	47.51	4.5	8.0	8.0
50	5 November 2010	36.06	139.84	45	36.14	4.6	8.2	8.2

that the energies at the three stations have a strong correlation. This reflects the fact that the ULF geomagnetic perturbations in the *H* component are dominated by external sources. In contrast, the *Z* component of geomagnetic fields at these three stations could be different from each other with the correlation coefficients as low as 0.72 (Figure 5d). This is probably because they are mainly induced fields which depend on not only external sources but also on local underground structures. However, as in Figure 5e, the energy of KAK is strongly correlatable with that of KNY, with a correlation coefficient of 0.94. Therefore, in this study, we chose the KNY station as a reference to remove the influences of global magnetic perturbations.

Table 3. List of Major Earthquakes With $E_s > 10^8$ in Region B

No.	DDMMYY	Latitude (°N)	Longitude (°E)	Depth (km)	Epicenter Distance (km)	Magnitude (JMA)	E_s' (lg)	E_s (lg)
1	25 February 2001	37.19	142.26	15	212.98	5.9	9.0	9.0
2	26 February 2001	37.16	142.27	27	212.19	5.5	8.4	8.4
3	17 April 2001	35.62	141.09	37	106.24	5.0	8.2	8.2
4	31 July 2001	36.09	141.66	43	133.51	5.1	8.2	8.2
5	4 September 2001	36.76	141.47	41	129.01	5.3	8.5	8.5
6	8 December 2001	37.15	139.96	5	104.54	4.9	8.1	8.2
7	19 June 2002	36.19	141.80	58	145.23	5.4	8.5	8.5
8	3 March 2003	37.69	141.78	41	215.33	5.9	9.0	9.0
9	8 April 2003	36.37	141.96	24	159.48	6.0	9.4	9.4
10	23 November 2003	35.58	141.13	39	111.89	5.1	8.3	8.3
11	21 August 2004	35.04	141.48	38	176.98	5.4	8.4	8.5
12	1 September 2004	36.92	141.78	31	161.77	5.6	8.8	8.8
13	17 October 2004	36.26	141.33	49	102.63	5.7	9.2	9.4
14	23 October 2004	37.29	138.87	13	166.42	6.8	10.6	10.8
15	24 October 2004	37.18	138.95	1	152.53	5.1	8.1	8.5
16	25 October 2004	37.33	138.95	15	164.56	5.8	9.1	9.2
17	27 October 2004	37.29	139.03	11	156.34	6.1	9.6	9.6
18	4 November 2004	37.43	138.92	18	174.70	5.2	8.1	8.1
19	6 November 2004	37.36	139.00	1	164.02	5.1	8.0	8.1
20	8 November 2004	37.40	139.03	1	165.24	5.9	9.2	9.3
21	10 November 2004	37.37	139.00	4	164.75	5.3	8.3	8.3
22	4 April 2005	37.37	141.75	43	188.64	5.3	8.2	8.2
23	19 May 2005	35.56	141.08	33	110.06	5.4	8.8	8.8
24	8 August 2005	36.34	141.45	46	113.57	5.6	9.0	9.0
25	22 October 2005	37.08	141.12	51	125.83	5.6	8.9	8.9
26	3 February 2006	36.25	141.48	52	115.79	4.9	7.9	8.2
27	13 March 2006	36.06	141.77	59	143.20	5.1	8.1	8.5
28	21 April 2006	34.94	139.20	7	169.18	5.8	9.0	9.1
29	2 May 2006	34.92	139.33	15	165.41	5.1	8.0	8.0
30	7 September 2006	35.59	141.06	38	106.06	5.1	8.3	8.3
31	20 June 2007	35.24	141.30	24	149.40	5.0	7.9	8.1
32	16 July 2007	37.56	138.61	16	203.34	6.8	10.4	10.4
33	21 September 2007	35.25	141.22	34	143.51	5.1	8.1	8.2
34	26 November 2007	37.30	141.76	44	183.82	6.0	9.2	9.2
35	9 February 2008	36.73	141.21	46	106.90	4.9	8.0	8.0
36	24 March 2008	37.12	141.45	47	149.65	5.3	8.4	8.4
37	2 May 2008	37.23	141.66	44	172.31	5.1	7.9	8.1
38	7 May 2008	36.25	141.88	24	152.03	5.0	7.9	8.2
39	8 May 2008	36.23	141.61	50	127.55	7.0	11.0	11.1
40	25 October 2008	36.00	141.63	46	132.27	5.0	8.0	8.1
41	20 December 2008	36.56	142.55	24	214.54	5.4	8.2	8.3
42	21 December 2008	36.60	142.47	1	208.08	6.2	9.5	9.5
43	24 December 2008	36.48	142.49	39	208.38	5.5	8.4	8.4
44	1 February 2009	36.72	141.28	47	111.62	5.8	9.3	9.3
45	21 April 2009	37.34	141.59	45	175.48	5.2	8.1	8.1
46	6 June 2009	35.54	141.26	42	123.76	5.9	9.4	9.4
47	1 September 2009	35.61	141.09	35	106.88	4.9	8.0	8.1
48	18 December 2009	34.96	139.13	4	170.61	5.1	8.0	8.0
49	13 June 2010	37.40	141.80	40	193.11	6.2	9.5	9.5
50	29 September 2010	37.28	140.03	7	117.96	5.7	9.2	9.2

4. Definition of ULF Geomagnetic Anomaly

To perform a statistical test of ULF seismomagnetic phenomena, one important thing is the selection of earthquake samples discussed in section 2. Another important thing is to identify and define geomagnetic anomalies. Because the energy correlation between KNY and KAK is very high for the Z component, we employ a linear least squares method to model the energy variation of KAK with the data of KNY:

$$\boldsymbol{Z}^*_{\mathrm{KAK}} = \beta \cdot \boldsymbol{Z}_{\mathrm{KNY}} + c \tag{3}$$

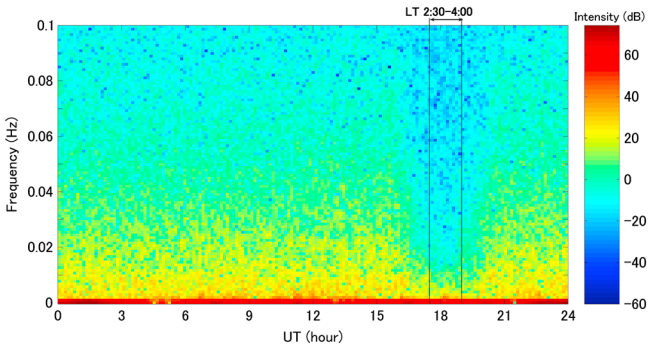

Figure 3. A typical spectrogram of the *Z* component of the geomagnetic data observed at KAK station.

where $\boldsymbol{Z}^*_{KAK}$ is the predicted daily energy at KAK station based on the energy observed at KNY station, $\boldsymbol{Z}_{KNY}$, during 2001–2010. Parameters β and c are the constant coefficients estimated by the least squares method:

$$\beta = \frac{n\sum \boldsymbol{Z}_{KNY}\boldsymbol{Z}_{KAK} - \sum \boldsymbol{Z}_{KNY}\sum \boldsymbol{Z}_{KAK}}{n\sum \boldsymbol{Z}_{KNY}{}^2 - \left(\sum \boldsymbol{Z}_{KNY}\right)^2} \tag{4}$$

$$c = \frac{\sum \boldsymbol{Z}_{KNY}{}^2 \sum \boldsymbol{Z}_{KAK} - \sum \boldsymbol{Z}_{KNY}\sum \boldsymbol{Z}_{KNY}\boldsymbol{Z}_{KAK}}{n\sum \boldsymbol{Z}_{KNY}{}^2 - \left(\sum \boldsymbol{Z}_{KNY}\right)^2} \tag{5}$$

where $\boldsymbol{Z}_{KAK}$ is the energy observed at KAK station; *n* is the total number of the 10 year daily energy data, which equals 3652 in this study.

As mentioned before, KNY station is located in an aseismic area. The energy variations of KNY are mostly related to global magnetic disturbances. Thus, the predicted energy variation based on these data could be roughly regarded as a reference model of such global geomagnetic changes at KAK station. In this way, the energy enhancements of the observed data at KAK station against its model could be taken as regional geomagnetic anomalies, which are possibly induced by underground activities. In order to quantify the energy enhancements, here we introduce a new parameter P, which is the ratio of the observed data $\boldsymbol{Z}_{KAK}$ to its model $\boldsymbol{Z}^*_{KAK}$:

$$P = \frac{\boldsymbol{Z}_{KAK}}{\boldsymbol{Z}^*_{KAK}} \tag{6}$$

Figure 6 gives an example of energy variations of the observed and modeled results at KAK, as well as the corresponding P values. In Figure 6a, the observed data, shown in green line, has very similar variations as the modeled data (red line), except for only a few data points. These exceptions have clearly been identified by their relative high P values, as shown in Figure 6b. Therefore, these high P values, which indicate regional energy enhancements, are employed to define magnetic anomalies.

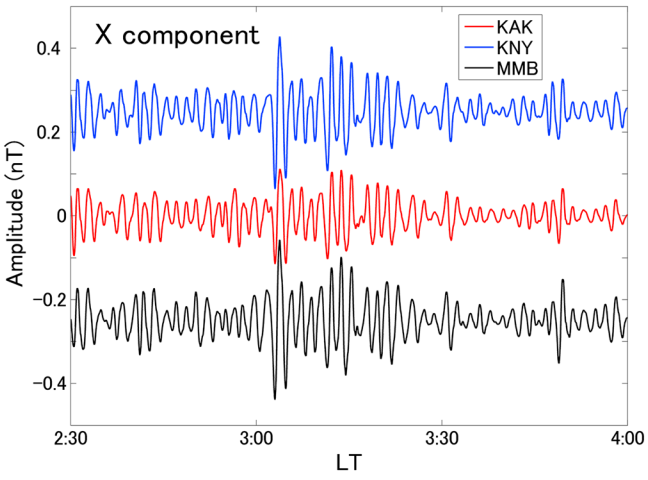

Figure 4. An example of wavelet transform results of the *X* component at KAK, KNY, and MMB stations. The central frequency of the signals is 0.01 Hz.

To find out a proper criterion for the anomaly definition, we check the empirical probability distribution of the 10 year P values. In Figure 7, most P values are around 1, implying that the modeled and observed results are usually similar. The conventional method to indentify anomaly data from a certain data set is using the mean + 2σ threshold. However, in Figure 7, it could be found

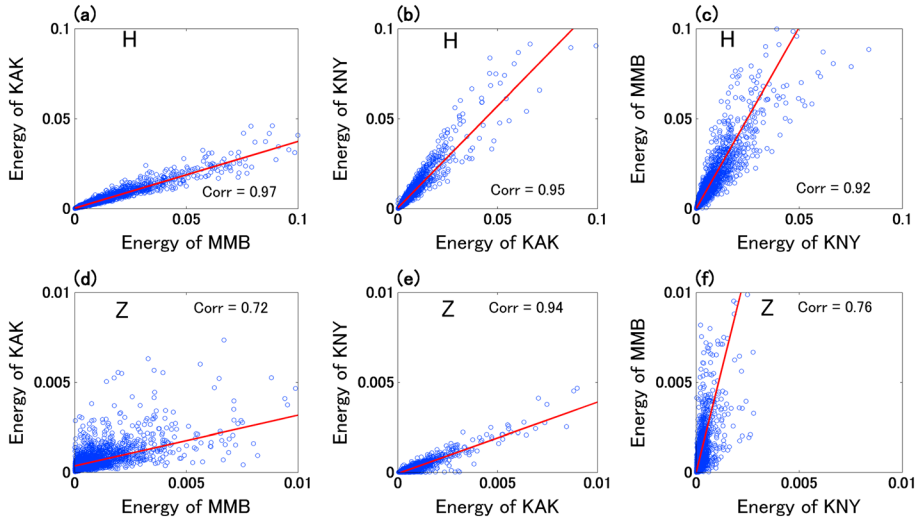

Figure 5. Correlations of 10 year daily energy of geomagnetic fields between two stations. The correlations for the *H* component: (a) MMB and KAK, (b) KAK and KNY, and (c) KNY and MMB. The correlations for the *Z* component: (d) MMB and KAK, (e) KAK and KNY, and (f) KNY and MMB. In each panel, Corr presents the correlation coefficient.

that the energy distributions are quasi-normal or skew, and the extremely large P values can seriously bias the mean and the σ. Therefore, here we utilize median and IQR (interquartile range), which are more robust estimations, to define the anomaly. For a normal distribution, the mean + 2σ value amounts to median + 1.5IQR [*Zwillinger and Kokoska*, 2000]. Thus, we define a geomagnetic anomaly when the value of P parameter exceeds median + 1.5IQR. As a result, there are 324 geomagnetic anomalies in total during 2001–2010.

5. Statistical Studies

5.1. Superposed Epoch Analysis

Although there have been accumulated reports on ULF seismomagnetic phenomena all over the world, the inside physics of these observed results are still unclear. Actually, the earthquake process is rather complex. There could be some geomagnetic anomalies originating from underground activities which are

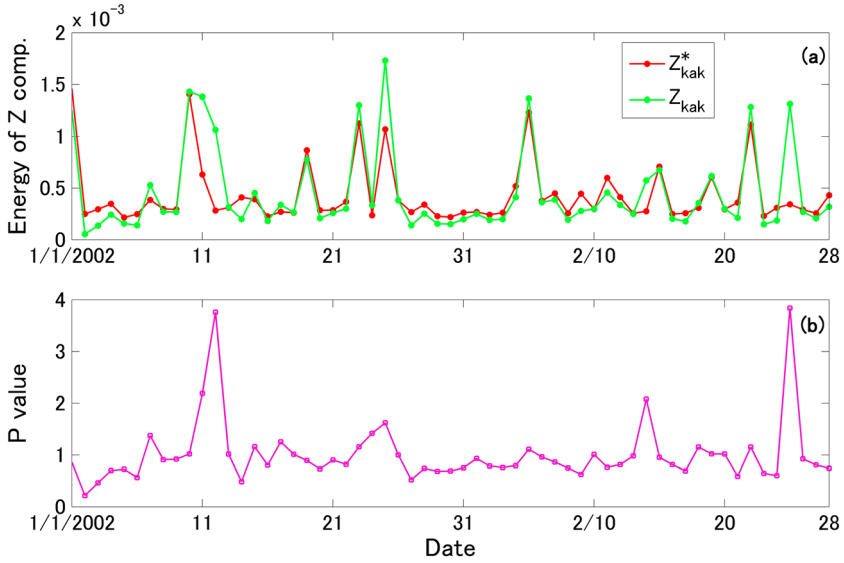

Figure 6. An example of energy variations and the corresponding P values of the *Z* component at KAK station. (a) The energy variations of observed data and modeled data by the green and the red lines, respectively. (b) The corresponding P values.

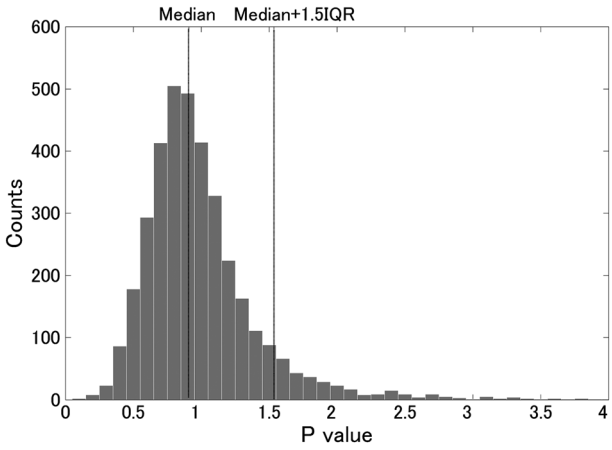

Figure 7. Histogram of 10 year P values. The vertical black broken lines indicate the median value and the median + 1.5IQR threshold.

not leading to large earthquakes, and there also could be some earthquakes which do not create geomagnetic anomalies. Therefore, we could not expect that the anomalies are one-to-one corresponding to earthquakes. This makes the seismomagnetic study rather complex and difficult. To verify the correlation between geomagnetic anomalies and local seismicity, statistical tests are required. In this section, statistical studies based on Superposed Epoch Analysis (SEA) have been performed at KAK station during 2001–2010. There are 50 earthquakes events and 324 geomagnetic anomalies during this period.

SEA is a statistical method to highlight a weak signal from noisy data. This technique can reveal typical characteristics, periodicities, and consequences of a special event [*Adams et al*., 2003; *Hocke*, 2008] and has been introduced in the studies of earthquake related GPS total electron content anomalies [*Kon et al*., 2011] and ULF geomagnetic anomalies [*Hattori et al*., 2013a]. In this paper, we apply SEA method to test ULF seismomagnetic phenomena at KAK, Japan. First, for each earthquake event, we create a data set of the P values for 45 days before and after its occurrence day. The time span of each data set is 91 days and centered at the event day. Next we investigate the anomalous P values as defined above. If the anomaly exists, we count one for the corresponding day. We repeat this procedure for all the selected 50 earthquake events, and we add up the counts for all data sets. We then obtain the SEA result in terms of the seismomagnetic anomaly. To evaluate the statistical significance, we randomly pick up 50 days from the entire analyzed period for KAK station instead of 50 earthquake days, and then perform the same procedure described above, to obtain the random SEA for ULF anomaly. We repeat such random SEA tests for 100,000 times to compute the mean (hereafter random_mean) and the corresponding standard deviation (σ).

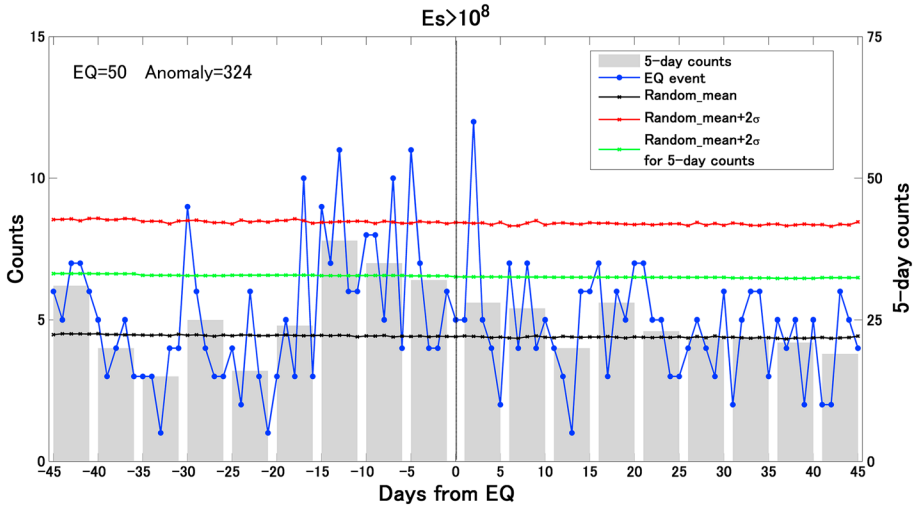

Figure 8. Results of ULF geomagnetic anomalies for Region A. The blue, the black, and the red lines demonstrate the counts of earthquake events, random_mean, and random_mean + 2σ, respectively. The gray bars and the green line show 5 day counts and corresponding random_mean + 2σ, respectively. Their values are given by the right vertical axis. Note that the count on the earthquake day is not included in the calculation of the 5 day counts. The vertical black broken line (the 0 day) indicates the day when E_s parameter is greater than 10^8.

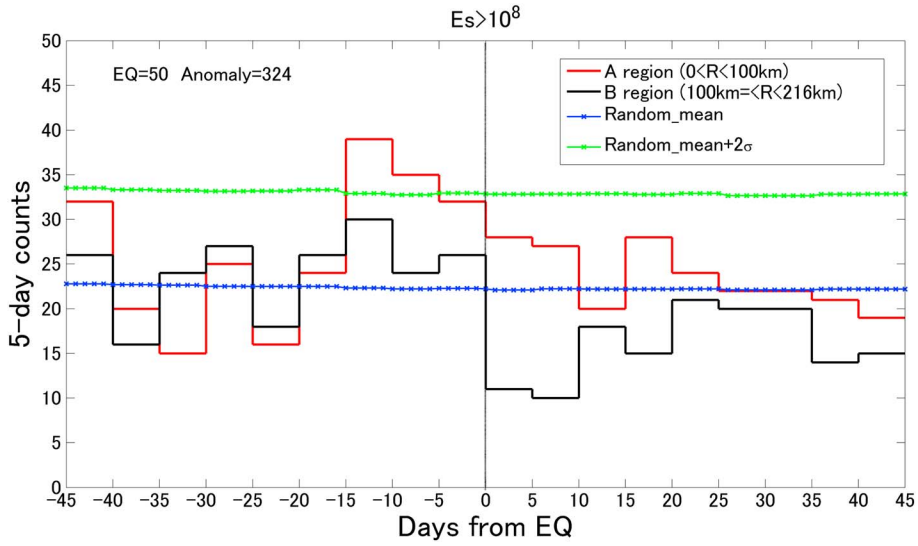

Figure 9. The 5 day counts for Regions A and B. The red and the black lines demonstrate the results of the 5 day counts for Regions A and B, respectively. The blue and the green lines show random_mean and random_mean + 2σ, respectively. Note that the count on the earthquake day is not included in the calculation of the 5 day counts. The vertical black broken line (the 0 day) indicates the day when E_s parameter is greater than 10^8.

Figure 8 shows the statistical results of ULF geomagnetic anomalies for Region A. The blue, black, and red lines show the counts of earthquake events, random_mean, and random_mean + 2σ, respectively. The gray bars and green line show 5 day counts and corresponding random_mean + 2σ, with their values given by the right vertical axis of the graph. A vertical black broken line (the 0 day) indicates the day when E_s parameter is greater than 10^8. In Figure 8, the number of count on a certain day indicates the number of earthquake events which are accompanied by geomagnetic anomalies on the day. Generally, if the earthquake events and the geomagnetic anomalies have no correlation, the counts probably distribute randomly and may not exceed the significant level. On the other hand, if the count on a certain day exceeds the random_mean + 2σ level, the ULF geomagnetic anomaly on this day will have a statistical significance, which suggests a possible correlation between the earthquakes and the geomagnetic anomalies. In Figure 8, before an adequate earthquake event, there are clearly higher probabilities of ULF anomalies than after the event. For KAK station, 30 days before, about 2 weeks before, few days before, and 2 days after, the event in Region A statistical results of daily counts are significant. Statistical results of 5 day counts show clear significance during the periods 6–15 days prior to the earthquake. These results are highly suggestive of the correlation between the earthquake events in Region A and the geomagnetic anomalies at KAK station.

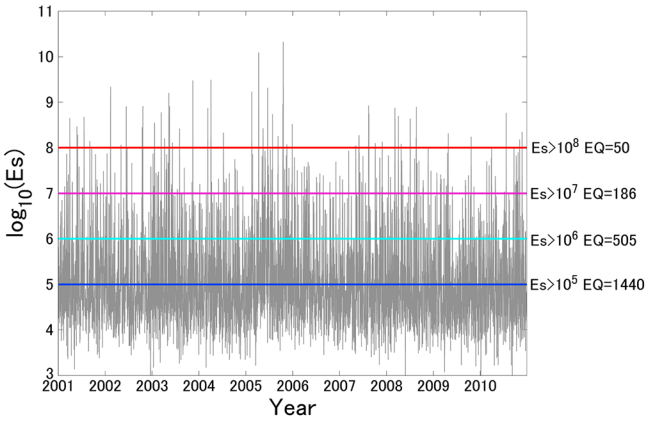

Figure 10. The E_s variation in Region A during 2001–2010. The numbers of earthquake events for E_s thresholds 10^5, 10^6, 10^7, and 10^8 are 1440, 505, 186, and 50, respectively.

5.2. The Dependence on Epicenter Distance (*R*)

Furthermore, to investigate whether the occurrence of the seismomagnetic anomalies depends on the epicenter distance, similar SEA has been applied in Region B. Here the number of earthquake events is also 50, and the number of geomagnetic anomalies is 324, which are the same as the ones used in Region A. Considering that the results of the 5 day counts are more stable and can provide more general characteristics of the data, hereafter we mainly discuss the results of 5 day counts.

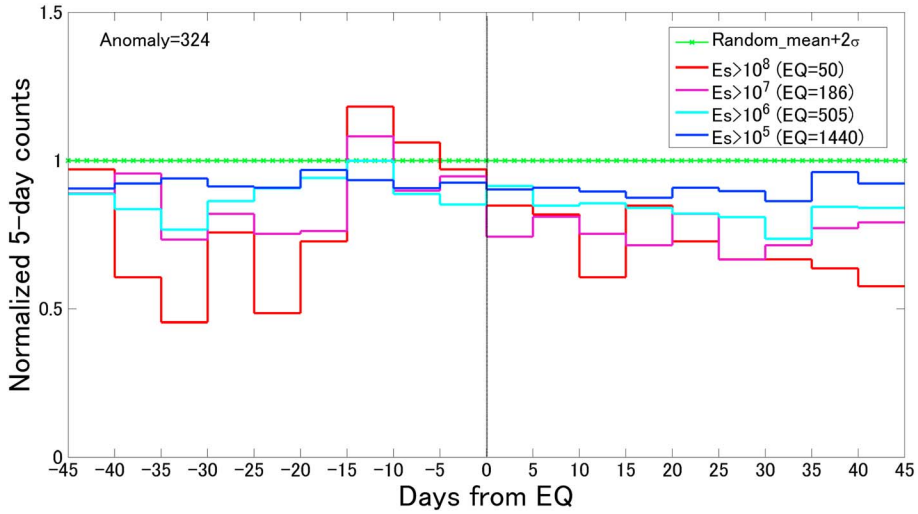

Figure 11. The 5 day counts for different E_s thresholds. The blue, the pale blue, the purple, and the red lines demonstrate the results of the 5 day counts for the E_s thresholds 10^5, 10^6, 10^7, and 10^8, respectively. The green line gives the random_mean + 2σ threshold. Note that the count on the earthquake day is not included in the calculation of the 5 day counts. The 5 day count values are normalized by the corresponding random_mean + 2σ for each E_s threshold. The vertical black broken line (the 0 day) indicates the day when E_s parameter exceeds the threshold.

For comparison, Figure 9 plots the 5 day counts of Regions A and B simultaneously. The blue and green lines show the random_mean and random_mean + 2σ, respectively. These two values are identical for Regions A and B, because there are equal numbers of earthquake events and geomagnetic anomalies. In Figure 9, significant anomalies are found within 6–15 days before the earthquake events in Region A, while there are no such clear anomalies in Region B. These results suggest that the ULF geomagnetic anomalies observed at KAK station are more likely to be related to closer earthquake events in Region A rather than farther events in Region B. In other words, the ULF seismomagnetic anomalies are more sensitive to closer earthquakes and are dependent on the epicenter distance.

5.3. The Dependence on Earthquake Energy (E_s)

In Figure 8, there is a clear statistical significance of ULF geomagnetic anomalies in relation to earthquake events with $E_s > 10^8$. To investigate the dependence on earthquake energy (E_s), here we apply a similar SEA with earthquake events selected by different E_s thresholds. Figure 10 gives the E_s variation in Region A during 2001–2010. The background E_s value is around 10^5. Therefore, we start to set several E_s thresholds between this value and 10^8 (i.e., 10^5, 10^6, 10^7, and 10^8). The number of earthquake events for each threshold is 1440, 505, 186, and 50, respectively. The results are shown in Figure 11. Although geomagnetic anomalies for each case are exactly the same here, the random_mean and random_mean + 2σ values differ, because the number of earthquake events varies. For comparison, we normalize the 5 day counts using the corresponding random_mean + 2σ. In Figure 11, the random_mean + 2σ values for each different E_s parameters are set as 1. Thus, if the 5 day counts are more than the corresponding random_mean + 2σ values, the normalized value will be more than 1; otherwise, it will be less than 1. It is found that there is no statistical significance in the results of background E_s value (10^5), shown by the blue line. With increasing the E_s value, the statistical results gradually approach to ($E_s = 10^6$) and finally exceed ($E_s = 10^7$ and $E_s = 10^8$) the threshold. This trend suggests that, only before earthquake events with large E_s index ($E_s >= 10^7$), there are statistical significances of ULF geomagnetic anomalies, which indicates that the occurrence of ULF geomagnetic anomalies depends on the E_s of the subsequent earthquake events.

6. Discussion

6.1. Parameter Selection

In a statistical test of ULF seismomagnetic phenomena, crucial points are how to select earthquakes and how to define ULF magnetic anomalies. These points lead to the following two challenges in ULF seismomagnetic

study: (1) the determinants of the detectability of ULF seismomagnetic signals for a given magnetic station and (2) identification of seismomagnetic signals from a noisy background.

Considering the skin effect of electromagnetic signals, usually, we only discuss earthquakes above a certain depth. In general, the probabilities of detection of earthquake-related ULF magnetic signals are higher for shallower, larger, and closer earthquakes [*Hattori*, 2004; *Hattori et al*., 2013a; *Zhuang et al*., 2005; *Schekotov et al*., 2007]. To quantify such influences of earthquake size and hypocenter distance, here we employ E_s parameter, which considers these influences simultaneously. The advantages of using E_s parameter are the following: (1) moderate earthquakes but very close to magnetic stations can be taken into account and (2) double counting of the same data set in SEA can be avoided when there are several adequate earthquakes occurring on the same day. Using E_s parameter, we have found a statistical significance of ULF geomagnetic anomalies about 6–15 days before local sizable earthquakes. Moreover, there is a clear E_s dependence in such statistical results. These suggest that the E_s parameter is reasonable and suitable for earthquake event selection in ULF seimomagnetic studies.

To identify the earthquake-related magnetic signals, a few methods have been taken in this study. First, we only utilized the data during nighttime (02:30–04:00 LT) to minimize the influences of artificial noise. Second, we employed a linear least squares method to estimate the global disturbances at KAK station using the data of the reference KNY station, based on their high correlation of 10 year daily energy. Ideally, it is better to estimate the linear coefficient using the data when there is no earthquake close to either KAK or KNY station, because uncorrelated outliers resulting from possible seismomagnetic signals could bias the estimation. However, it is very difficult to find a "clean" period, especially for KAK station located in a seismically active area. To assure the bias, the method of iteratively reweighted least squares (IRLS) is also employed. IRLS is used to find the maximum likelihood estimates of a generalized linear model, as a way of mitigating the influence of outliers [*Ke and Kanade*, 2005]. The linear coefficients β and c in equation (3) obtained by linear least squares and by IRLS are almost the same, which suggests that the bias is negligible. Finally, we defined a new parameter, the P value, by the ratio of the observed energy to its model at KAK to remove the influences of global geomagnetic disturbances. This new parameter could reflect the local energy enhancements at KAK station effectively. The probability distribution of the P value during 2001–2010 is skew. Therefore, we use a robust estimation of median + 1.5IQR as the criterion of P value to define ULF geomagnetic anomaly.

6.2. The Efficiency of ULF Seismomagnetic Phenomena for Earthquake Forecasting

In Figure 8, there are clear statistical significances of ULF geomagnetic anomalies a few days before sizable earthquakes. These anomalies could be used to forecast subsequent earthquakes. For example, if we use the anomalies on −5 day and predict earthquakes to happen 5 days later within 100 km from KAK station, 22% (11 out of 50) sizable earthquakes will be detected. The ratio will increase when the alarm window becomes longer. The alarm window is the period during which an alarm is valid. On the other hand, the ratio of false alarm will also increase when more alarms are issued. Thus, the Molchan's error diagram [*Molchan*, 1991] is introduced to evaluate the efficiency of ULF geomagnetic anomalies for local earthquake forecasting.

Molchan's error diagram plots the rate of earthquakes missed against the rate of alarmed cells. In application, the threshold for issuing an alarm would be selected via retrospective analysis. The probability gain, which is the ratio of detecting rate to alarm rate, indicates how many times more information than a random guess (a Poisson model) [*Molchan*, 1991; *Zechar and Jordan*, 2008]. Recently, this method has been applied in the study of short-term earthquake forecasting based on GPS data [*Wang et al*., 2013], and more details for Molchan's error diagram could be found there. In this study, we apply similar analysis using ULF geomagnetic data to predict earthquakes in Region A. In Figure 8, the most prominent result of 5 day counts is found to be 11–15 days prior to sizable earthquakes. Therefore, here the leading time (Δ) is set as 11 days, and the alarm window (L) is set as 5 days, so that an earthquake can be alarmed if there is any geomagnetic anomaly 11–15 days before. Figure 12 gives the Molchan's error diagram using the geomagnetic anomalies as precursors. The horizontal axis gives proportion of alarmed cells, and vertical axis gives proportion of earthquakes missed. A black dashed line through the diagonal indicates the prediction by random guess; a black solid line shows the prediction based on ULF geomagnetic anomalies. Generally, the proportion of unpredicted earthquakes goes down with the increasing of alarmed cells. For a Poisson model, if we make alarm randomly, the proportion of predicted earthquakes will be equal to the proportion of alarmed cells, which is demonstrated by the black broken diagonal line in Figure 12. Any prediction above this line indicates that the proportion of predicted earthquakes is less than that of alarmed cells, implying that the prediction

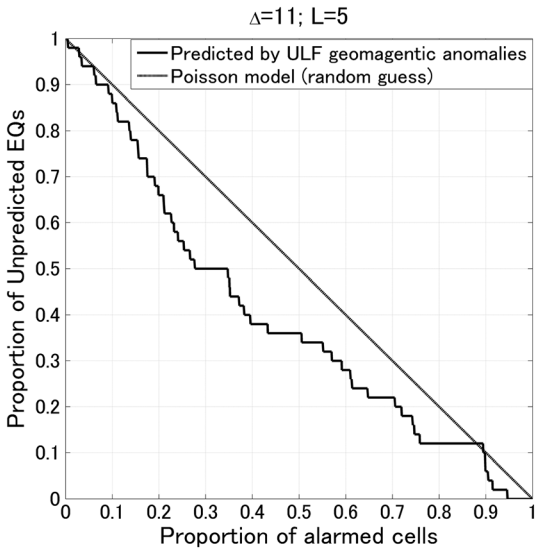

Figure 12. Molchan's error diagram for earthquake predictions using the geomagnetic anomalies as precursors in Region A. The leading time (Δ) is set as 11 days, and the alarm window (*L*) is set as 5 days. The black broken line gives the results of random guess; the black solid line presents the results of prediction based on ULF geomagnetic anomalies.

is worse than random guess. Otherwise, if below the diagonal line, the prediction is better than random guess. Figure 12 shows that the prediction by ULF geomagnetic anomalies is obviously better than random guess with a probability gain around 1.6 against a Poisson model. These results suggest that the ULF geomagnetic anomalies do contain precursory information of local sizable earthquakes and have potential capability to improve short-term earthquake forecasting.

6.3. Implications and Further Studies

Since the end of last century, ULF seismomagnetic phenomena have been intensively studied. It was once considered as a promising candidate for short-term earthquake prediction, because a number of successful case studies had been reported. However, there are still active debates in the geophysical community on the seismoelectromagnetic phenomena. The correlation between magnetic anomalies and seismicity has been queried. Moreover, there are two essential problems puzzling the researchers: (1) what is the exact waveform of electromagnetic signals associated with earthquakes or underground activities and (2) how are the signals generated. Until now, these two questions have not yet been answered clearly or fully.

To date, most ULF seismomagnetic studies focus on detecting precursors of large earthquakes using different approaches. However, to verify, clarify, and evaluate the ULF seismomagnetic phenomena, statistical studies based on continuous long-term monitoring of ULF magnetic field in a seismically active area is required. In this study, we have utilized the data of KAK station operated by JMA to perform such statistical tests. The results suggest a correlation between magnetic anomalies and local seismicity. Therefore, this study has made a dent in verifying the ULF seismomagnetic phenomena. For a further understanding, we need to apply waveform analysis to clarify the signals associated with earthquakes and other underground activities. Indoor experiments and numerical simulations based on the waveforms of observed seimomagnetic signals are also useful for understanding the mechanisms. These further studies are expected to shed light on the siemomagnetic phenomena.

7. Conclusion

In order to verify the existence of ULF electromagnetic phenomena preceding large earthquakes, statistical studies based on SEA have been applied to the data observed at KAK, Japan, during 2001–2010. First, the E_s parameter is employed to select the earthquake events. And then, a new parameter P value, which reflects the local energy enhancements at KAK station, is introduced to define geomagnetic anomalies. The results of SEA indicate that, before a sizable earthquake event ($E_s > 10^8$), there are clearly higher probabilities of ULF anomalies than that after the event: statistical results of daily counts are found significant at 30 days before, about 2 weeks before, few days before, and 2 days after the event; statistical results of 5 day counts are found significant at the period 6–15 days before. These results are quite similar to those of previous statistical studies in Izu and Boso Peninsulas, Japan, reported by *Hattori et al.* [2013a]. Moreover, this study have shown clear E_s (earthquake energy) and R (epicenteral distance) dependences, which suggest that the ULF geomagnetic anomalies at KAK station are more sensitive to larger and closer events, respectively. Further investigations by Molchan's error diagram suggest that the ULF seismomagnetic phenomena obtained at KAK do contain precursory information and have potential capability to improve forecasting of large earthquakes. Therefore, we conclude that the ULF geomagnetic observation is useful and important for local earthquake forecasting. The mechanisms of ULF seismomagnetic phenomena and the detailed waveform of earthquake-related geomagnetic signals are worthwhile being studied in future.

Acknowledgments
The authors would like to thank the Japan Meteorological Agency for providing geomagnetic data and earthquake catalogs. This research is partly supported by the Grand-in-Aid for Scientific Research of Japan Society for Promotion of Science (19403002) and National Institute of Information and Communication Technology (research and development promotion funding international joint research).

Alan Rodger thanks Clark Dunson and an anonymous reviewer for their assistance in evaluating this paper.

References

Adams, J. B., M. E. Mann, and C. M. Ammann (2003), Proxy evidence for an El Niño-like response to volcanic forcing, *Nature*, *426*, 274–278.
Akhoondzadeh, M., M. Parrot, and M. R. Saradjian (2010), Electron and ion density variations before strong earthquakes (M > 6.0) using DEMETER and GPS data, *Nat. Hazards Earth Syst. Sci.*, *10*, 7–18, doi:10.5194/nhess-10-7-2010.
Campbell, W. H. (2009), Natural magnetic disturbance fields, not precursors preceding the Loma Prieta earthquake, *J. Geophys. Res.*, *114*, A05307, doi:10.1029/2008JA013932.
Chavez, O., J. P. Millan-Almaraz, R. Pérez-Enríquez, J. A. Arzate-Flores, A. Kotsarenko, J. A. Cruz-Abeyro, and E. Rojas (2010), Detection of ULF geomagnetic signals associated with seismic events in Central Mexico using Discrete Wavelet Transform, *Nat. Hazards Earth Syst. Sci.*, *10*, 2557–2564, doi:10.5194/nhess-10-2557-2010.
Chen, C. H., J. Y. Liu, P. Y. Lin, H. Y. Yen, K. Hattori, W. T. Liang, Y. I. Chen, Y. H. Yeh, and X. Zeng (2010), Pre-seismic geomagnetic anomaly and earthquake location, *Tectonophysics*, *489*, 240–247, doi:10.1016/j.tecto.2010.04.018.
Chen, C. H., et al. (2013), Evaluation of seismo-electric anomalies using magnetic data in Taiwan, *Nat. Hazards Earth Syst. Sci.*, *13*, 597–604, doi:10.5194/nhess-13-597-2013.
Enomoto, Y. (2012), Coupled interaction of earthquake nucleation with deep Earth gases: A possible mechanism for seismo-electromagnetic phenomena, *Geophys. J. Int.*, *191*, 1210–1214, doi:10.1111/j.1365-246X.2012.05702.x.
Fraser-Smith, A. C., A. Bernardi, P. R. McGill, M. E. Ladd, R. A. Helliwell, and O. G. Villard (1990), Low-frequency magnetic field measurements near the epicenter of the Ms 7.1 Loma Prieta earthquake, *Geophys. Res. Lett.*, *17*, 1465–1468, doi:10.1029/GL017i009p01465.
Freund, F. (2000), Time-resolved study of charge generation and propagation in igneous rocks, *J. Geophys. Res.*, *105*, 11,001–11,019, doi:10.1029/1999JB900423.
Freund, F. (2002), Charge generation and propagation in rocks, *J. Geodyn.*, *33*, 545–572.
Galperin, Y. I., and M. Hayakawa (1996), On the magnetospheric effects of experimental explosions observed from AUREOL-3, *J. Geomagn. Geoelectr.*, *48*, 1241–1263.
Gokhberg, M. B., V. A. Morgounov, T. Yoshino, and I. Tomizawa (1982), Experimental measurement of electromagnetic emissions possibly related to earthquakes in Japan, *J. Geophys. Res.*, *87*, 7824–7828, doi:10.1029/JB087iB09p07824.
Han, P. (2013), Investigation of ULF seismo-magnetic phenomena in Kanto, Japan during 2000–2010, PhD thesis, Chiba University, Chiba, Japan.
Han, P., Q. H. Huang, and J. G. Xiu (2009), Principle component analysis of geomagnetic diurnal variation associated with earthquakes: Case study of the M6.1 Iwateken Nairiku Hokubu earthquake, *Chin. J. Geophys.*, *52*(6), 1556–1563, doi:10.3969/j.issn.0001-5733.2009.06.017.
Han, P., K. Hattori, Q. Huang, T. Hirano, Y. Ishiguro, C. Yoshino, and F. Febriani (2011), Evaluation of ULF electromagnetic phenomena associated with the 2000 Izu Islands earthquake swarm by wavelet transform analysis, *Nat. Hazards Earth Syst. Sci.*, *11*, 965–970, doi:10.5194/nhess-11-965-2011.
Hattori, K. (2004), ULF geomagnetic changes associated with large earthquakes, *Terr. Atmos. Oceanic Sci.*, *15*, 329–360.
Hattori, K., et al. (2004a), ULF geomagnetic field measurements in Japan and some recent results associated with Iwateken Nairiku Hokubu earthquakes in 1998, *Phys. Chem. Earth*, *29*, 481–494, doi:10.1016/j.pce.2003.09.019.
Hattori, K., A. Serita, K. Gotoh, C. Yoshino, M. Harada, N. Isezaki, and M. Hayakawa (2004b), ULF geomagnetic anomaly associated with 2000 Izu islands earthquake swarm, Japan, *Phys. Chem. Earth*, *29*, 425–436, doi:10.1016/j.pce.2003.11.014.
Hattori, K., A. Serita, C. Yoshino, M. Hayakawa, and N. Isezaki (2006), Singular spectral analysis and principal component analysis for signal discrimination of ULF geomagnetic data associated with 2000 Izu Island Earthquake Swarm, *Phys. Chem. Earth*, *31*, 281–291, doi:10.1016/j.pce.2006.02.034.
Hattori, K., P. Han, C. Yoshino, F. Febriani, H. Yamaguchi, and C. Chen (2013a), Investigation of ULF seismo-magnetic phenomena in Kanto, Japan during 2000–2010: Case studies and statistical studies, *Surv. Geophys.*, *34*, 293–316.
Hattori, K., P. Han, and Q. Huang (2013b), Global variation of ULF geomagnetic fields and detection of anomalous changes at a certain observatory using reference data, *Electr. Eng. Jpn.*, *182*, 9–18, doi:10.1002/eej.22299.
Hayakawa, M. (1999), *Atmospheric and Ionospheric Electromagnetic Phenomena Associated With Earthquakes*, TERRAPUB, Tokyo, Japan.
Hayakawa, M., and O. A. Molchanov (2002), *Seismo Electromagnetic: Lithosphere–Atmosphere–Ionosphere Coupling*, TERRAPUB, Tokyo, Japan.
Hayakawa, M., R. Kawate, O. A. Molchanov, and K. Yumoto (1996a), Results of ultra-low-frequency magnetic field measurements during the Guam earthquake of 8 August 1993, *Geophys. Res. Lett.*, *23*, 241–244, doi:10.1029/95GL02863.
Hayakawa, M., O. A. Molchanov, T. Ondoh, and E. Kawai (1996b), Anomalies in the subionospheric VLF signals for the 1995 Hyogoken Nanbu earthquake, *J. Phys. Earth*, *44*, 413–418.
Hirano, T., and K. Hattori (2011), ULF geomagnetic changes possibly associated with the 2008 Iwate–Miyagi Nairiku earthquake, *J. Asian Earth Sci.*, *41*, 442–449, doi:10.1016/j.jseaes.2010.04.038.
Hocke, K. (2008), Oscillations of global mean TEC, *J. Geophys. Res.*, *113*, A04302, doi:10.1029/2007JA012798.
Huang, Q. H. (2002), One possible generation mechanism of co-seismic electric signals, *Proc. Jpn. Acad., Ser. B*, *78*(B7), 173–178.
Huang, Q. H. (2005), Controlled analogue experiments on propagation of seismic electromagnetic signals, *Chin. Sci. Bull.*, *50*, 1956–1961.
Huang, Q. H. (2011a), Rethinking earthquake-related DC-ULF electromagnetic phenomena: Towards a physics-based approach, *Nat. Hazards Earth Syst. Sci.*, *11*, 2941–2949, doi:10.5194/nhess-11-2941-2011.
Huang, Q. H. (2011b), Retrospective investigation of geophysical data possibly associated with the Ms8.0 Wenchuan earthquake in Sichuan, China, *J. Asian Earth Sci.*, *41*, 421–427, doi:10.1016/j.jseaes.2010.05.014.
Huang, Q. H., and Y. F. Lin (2010), Selectivity of seismic electric signal (SES) of the 2000 Izu earthquake swarm: A 3D FEM numerical simulation model, *Proc. Jpn. Acad., Ser. B*, *86*(3), 257–264, doi:10.2183/pjab.86.257.
Jach, A., P. Kokoszka, J. Sojka, and L. Zhu (2006), Wavelet-based index of magnetic storm activity, *J. Geophys. Res.*, *111*, A09215, doi:10.1029/2006JA011635.
Johnston, M. (1997), Review of electric and magnetic fields accompanying seismic and volcanic activity, *Surv. Geophys.*, *18*, 441–476, doi:10.1023/A:1006500408086.
Kappler, K. N., H. F. Morrison, and G. D. Egbert (2010), Long-term monitoring of ULF electromagnetic fields at Parkfield, California, *J. Geophys. Res.*, *115*, B04406, doi:10.1029/2009JB006421.
Kawate, R., O. A. Molchanov, and M. Hayakawa (1998), Ultra-lowfrequency magnetic fields during the Guam earthquake of 8 August 1993 and their interpretation, *Phys. Earth Planet. Inter.*, *105*, 229–238.
Ke, Q., and T. Kanade (2005), Robust L1 norm factorization in the presence of outliers and missing data by alternative convex programming, IEEE Conference on Computer Vision and Pattern Recognition (CVPR 2005), San Diego, Calif.
Kon, S., M. Nishihashi, and K. Hattori (2011), Ionospheric anomalies possibly associated with M≥ 6.0 earthquakes in the Japan area during 1998–2010: Case studies and statistical study, *J. Asian Earth Sci.*, *41*, 410–420, doi:10.1016/j.jseaes.2010.10.005.

Kopytenko, Y. A., T. G. Matishvili, P. M. Voronov, E. A. Kopytenko, and O. A. Molchanov (1993), Detection of ultra-low-frequency emissions connected with the Spitak earthquake and its aftershock activity, based on geomagnetic pulsations data at Dusheti and Vardzia observatories, *Phys. Earth Planet. Inter.*, *77*, 85–95.

Kopytenko, Y. A., T. G. Matishvili, P. M. Voronov, and E. A. Kopytenko (1994), Observation of electromagnetic ultra-low-frequency lithospheric emissions in the Caucasian seismically active zone and their connection with earthquakes, in *Electromagnetic Phenomena Related to Earthquake Prediction*, edited by M. Hayakawa and Y. Fujinawa, pp. 175–180, TERRAPUB, Tokyo, Japan.

Kopytenko, Y. A., V. Ismaguilov, K. Hattori, and M. Hayakawa (2006), Determination of hearth position of a forthcoming strong EQ using gradients and phase velocities of ULF geomagnetic disturbances, *Phys. Chem. Earth*, *31*, 292–298, doi:10.1016/j.pce.2006.02.004.

Lighthill, J. (1996), *A Critical Review of VAN*, 376 pp., World Scientific, Singapore.

Liu, J. Y., Y. I. Chen, Y. J. Chuo, and H. F. Tsai (2001), Variations of ionospheric total electron content during the Chi-Chi earthquake, *Geophys. Res. Lett.*, *28*, 1383–1386, doi:10.1029/2000GL012511.

Liu, J. Y., Y. I. Chen, Y. J. Chuo, and C. S. Chen (2006), A statistical investigation of preearthquake ionospheric anomaly, *J. Geophys. Res.*, *111*, A05304, doi:10.1029/2005JA011333.

Liu, J. Y., et al. (2009), Seismoionospheric GPS total electron content anomalies observed before the 12 May 2008 Mw 7.9 Wenchuan earthquake, *J. Geophys. Res.*, *114*, A04320, doi:10.1029/2008JA013698.

Masci, F. (2010), On claimed ULF seismogenic fractal signatures in the geomagnetic field, *J. Geophys. Res.*, *115*, A10236, doi:10.1029/2010JA015311.

Molchan, G. M. (1991), Structure of optimal strategies in earthquake prediction, *Tectonophysics*, *193*, 267–276.

Molchanov, O. A., and M. Hayakawa (1998), Subionospheric VLF signal perturbations possibly related to earthquakes, *J. Geophys. Res.*, *103*, 17,489–17,504, doi:10.1029/98JA00999.

Molchanov, O. A., Y. A. Kopytenko, P. M. Voronov, E. A. Kopytenko, T. G. Matiashvili, A. C. Fraser-Smith, and A. Bernardi (1992), Results of ULF magnetic field measurements near the epicenters of the Spitak (Ms = 6.9) and Loma Prieta (Ms = 7.1) earthquakes: Comparative analysis, *Geophys. Res. Lett.*, *19*, 1495–1498, doi:10.1029/92GL01152.

Molchanov, O. V., and M. Hayakawa (1995), Generation of ULF electromagnetic emissions by microfracturing, *Geophys. Res. Lett.*, *22*, 3091–3094, doi:10.1029/95GL00781.

Nagao, T., et al. (2002), Electromagnetic anomalies associated with 1995 Kobe earthquake, *J. Geodyn.*, *33*, 401–411.

Ouzounov, D., N. Bryant, T. Logan, S. Pulinets, and P. Taylor (2006), Satellite thermal IR phenomena associated with some of the major earthquakes in 1999–2004, *Phys. Chem. Earth*, *31*, 154–163.

Ouzounov, D., D. Liu, C. Kang, G. Cervone, M. Kafatos, and P. Taylor (2007), Outgoing long wave radiation variability from IR satellite data prior to major earthquakes, *Tectonophysics*, *431*, 211–220.

Ren, H., X. Chen, and Q. Huang (2012), Numerical simulation of co-seismic electromagnetic fields associated with seismic waves due to finite faulting in porous media, *Geophys. J. Int.*, *188*, 925–944, doi:10.1111/j.1365-246X.2011.05309.x.

Sarkar, S., A. K. Gwal, and M. Parrot (2007), Ionospheric variations observed by the DEMETER satellite in the mid-latitude region during strong earthquakes, *J. Atmos. Sol. Terr. Phys.*, *69*, 1524–1540, doi:10.1016/j.jastp.2007.06.006.

Schekotov, A. Y., O. A. Molchanov, M. Hayakawa, E. N. Fedorov, V. N. Chebrov, V. I. Sinitsin, E. E. Gordeev, G. G. Belyaev, and N. V. Yagova (2007), ULF/ELF magnetic field variations from atmosphere induced by seismicity, *Radio Sci.*, *42*, RS6S90, doi:10.1029/2005RS003441.

Telesca, L., and K. Hattori (2007), Non-uniform scaling behavior in Ultra Low Frequency (ULF) earthquake-related geomagnetic signals, *Physica A*, *384*, 522–528.

Telesca, L., V. Lapenna, M. Macchiato, and K. Hattori (2008), Investigating non-uniform scaling behavior in Ultra Low Frequency (ULF) earthquake-related geomagnetic signals, *Earth Planet. Sci. Lett.*, *268*, 219–224, doi:10.1016/j.epsl.2008.01.033.

Thomas, J., J. Love, and M. Johnston (2009), On the reported magnetic precursor of the 1989 Loma Prieta earthquake, *Phys. Earth Planet. Inter.*, *173*, 207–215, doi:10.1016/j.pepi.2008.11.014.

Tramutoli, V., V. Cuomo, C. Filizzola, N. Pergola, and C. Pietrapertosa (2005), Assessing the potential of thermal infrared satellite surveys for monitoring seismically active areas, The case of Kocaeli (İzmit) earthquake, August 17th, 1999, *Remote Sens. Environ.*, *96*, 409–426.

Uyeda, S., M. Hayakawa, T. Nagao, O. Molchanov, K. Hattori, Y. Orihara, K. Gotoh, Y. Akinaga, and H. Tanaka (2002), Electric and magnetic phenomena observed before the volcano-seismic activity in 2000 in the Izu Island Region, Japan, *Proc. Natl. Acad. Sci. U.S.A.*, *99*(11), 7352–7355.

Uyeda, S., M. Kamogawa, and H. Tanaka (2009), Analysis of electrical activity and seismicity in the natural time domain for the volcanic-seismic swarm activity in 2000 in the Izu Island region, Japan, *J. Geophys. Res.*, *114*, B02310, doi:10.1029/2007JB005332.

Varotsos, P., and K. Alexopoulos (1984), Physical-properties of the variations of the electric-field of the earth preceding earthquakes, *Tectonophysics*, *110*, 73–98, doi:10.1016/0040-1951(84)90059-3.

Varotsos, P., and M. Lazaridou (1991), Latest aspects of earthquake prediction in Greece based on seismic electric signals, *Tectonophysics*, *188*, 321–347.

Wang, T., J. Zhuang, T. Kato, and M. Bebbington (2013), Assessing the potential improvement in short-term earthquake forecasts from incorporation of GPS data, *Geophys. Res. Lett.*, *40*, 2631–2635, doi:10.1002/grl.50554.

Wen, S., C. H. Chen, H. Y. Yen, T. K. Yeh, J. Y. Liu, K. Hattori, P. Han, C. H. Wang, and T. C. Shin (2012), Magnetic storm free ULF analysis in relation with earthquakes in Taiwan, *Nat. Hazards Earth Syst. Sci.*, *12*, 1747–1754, doi:10.5194/nhess-12-1747-2012.

Xu, G., P. Han, Q. Huang, K. Hattori, F. Febriani, and H. Yamaguchi (2013), Anomalous behaviors of geomagnetic diurnal variations prior to the 2011 off the Pacific coast of Tohoku earthquake (Mw9.0), *J. Asian Earth Sci.*, *77*, 59–65, doi:10.1016/j.jseaes.2013.08.011.

Yen, H., C. Chen, Y. Yeh, J. Liu, C. Lin, and Y. Tsai (2004), Geomagnetic fluctuations during the 1999 Chi-Chi earthquake in Taiwan, *Earth Planets Space*, *56*, 39–45.

Yoshida, S., M. Uyeshima, and M. Nakatani (1997), Electric potential changes associated with a slip failure of granite: Preseismic and coseismic signals, *J. Geophys. Res.*, *102*, 14,883–14,897, doi:10.1029/97JB00729.

Zechar, J. D., and T. H. Jordan (2008), Testing alarm-based earthquake predictions, *Geophys. J. Int.*, *172*, 715–724.

Zhao, G., Y. Zhan, L. Wang, J. Wang, J. Tang, Q. Xiao, and X. Chen (2009), Electromagnetic anomaly before earthquakes measured by electromagnetic experiments, *Earthquake Sci.*, *22*, 395–402, doi:10.1007/s11589-009-0395-5.

Zhuang, J., D. Vere-Jones, H. Guan, Y. Ogata, and L. Ma (2005), Preliminary analysis of observations on the ultra-low frequency electric field in a region around Beijing, *Pure Appl. Geophys.*, *162*, 1367–1396, doi:10.1007/s00024-004-2674-3.

Zwillinger, D., and S. Kokoska (2000), *CRC Standard Probability and Statistics Tables and Formulae*, CRC Press, Boca Raton, Fla.